Light Entanglement via Four Wave Mixing through a Rubidium Vapor Cell

Haley Bauser

Advisor: Irina Novikova

The College of William & Mary, Physics Department

April 15, 2016

Abstract

Light entanglement holds the potential for quantum telecommunication and quantum computing. The goal of the project is to produce a pair of polarization-entangled light fields using Four Wave Mixing (FWM) in hot Rb vapor. In this process interaction of atoms with near-resonant strong control optical field results in strong amplification of a probe optical field and in generation of a quantum correlated conjugate Stokes optical field. The optimum parameters for FWM have been established. Through analysis of the noise, the RF settings allowing for experimental quantum noise to match the shot noise has been confirmed as well. After establishing the shot noise limit, there were many trials to achieve noise lower than the shot noise. To further improve the noise and thus establish the quantum correlation between our fields, we switched from a single laser to a double laser setup. In the future, the quantum correlation between the Stokes field and the probe field will be further improved to allow for the entangled Bell states creation.

Contents

List of Figures

1 Introduction

1.1 Motivation

Light entanglement is central in current research involving quantum information and improvement of quantum sensor technologies. Entanglement occurs when pairs of particles cannot be characterized independently, and instead, exist in a quantum state in a superimposed form as given by the following equation:

$$|\Psi\rangle_{1,2} = \frac{1}{\sqrt{2}}(|\uparrow\rangle|\downarrow\rangle \pm |\downarrow\rangle|\uparrow\rangle) \tag{1}$$

However, when a measurement is made on one particle, the superposition of states collapses thus breaking the entanglement. However, based on the knowledge about one of the states gained from the measurement, information is immediately known about the other state. For example, if there exists a quantum state with spins +1/2 and spin -1/2 and a total spin of 0, by taking a measurement of the system the system collapses. However, if your measurement yielded a spin of +1/2, you know that the other spin value was -1/2 thus completes an instant transfer of information. This property gives potential for qubits, in which information is stored as a superposition of two states at once, and would be much more efficient than classical computing systems. Through this phenomenon comes the potential for quantum information telecommunication and the increase of measurement accuracy through quantum sensor technologies. Here we report the progress toward realization of polarization entangled optical fields. This work is motivated by the experiment in nonlinear crystals that found correlations in higher orders of polarization states [1].

1.2 Four Wave Mixing

In our project, we will be generating the entangled quantum Bell states [2], an example of which is given by Equations 1 and 2. Entanglement, by nature, cannot be induced

simply through one beam. We will be using the pair of two quantum correlated optical field generated in the process of Four Wave Mixing (FWM). This method has previously been effective in both optical fibers and atomic vapors. FWM is induced when a strong control laser field propagates through a ensemble of three-level atoms [3], (as shown in Fig.1). When another weak optical probe field (at a different frequency) interacts with the same atoms, a correlated third field is produced, formed by the scattering of the incident photons.

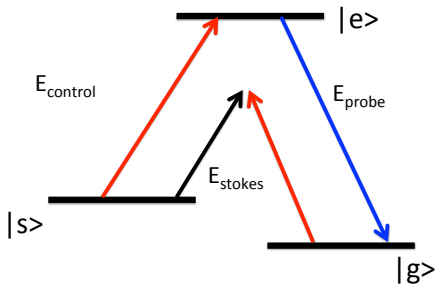

Figure 1: FWM Double Lambda Energy Configuration

In Figure 1, the horizontal black lines represent the different atomic energy states where $|s\rangle$ and $|g\rangle$ are the hyperfine components of the ground electronic state, and $|e\rangle$ is the excited electronic state. The red lines represent the control optical field. The blue arrow is the seeded probe optical field. The black arrow represents our created correlated signal, or Stokes field.

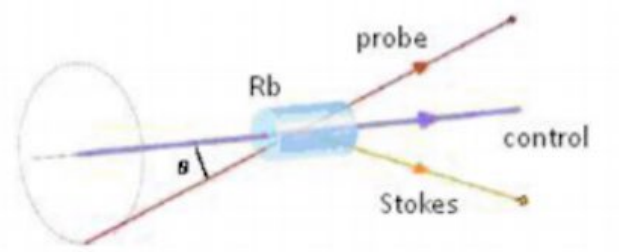

Figure 2: FWM through Rubidium vapor cell

Figure 2 shows more practically how Four Wave Mixing is produced within our Rubidium vapor cell

FWM is the optimal way to produce the frequency and intensity correlated pairs of beams and a necessary first step in creation of Bell States. By mixing such quantum optical fields

with various polarizations, it is possible to entangle frequency and polarizations modes to realize all four polarization-frequency optical Bell states. The Bell states are given in the following equations:

$$\begin{aligned} &\frac{1}{\sqrt{2}}(|H\rangle_P|H\rangle_S \pm |V\rangle_P|V\rangle_S) \\ &\frac{1}{\sqrt{2}}(|H\rangle_P|V\rangle_S \pm |V\rangle_P|H\rangle_S) \end{aligned} \tag{2}$$

1.3 Use of Rubidium

More traditionally, correlated photon pairs in similar quantum entanglement experiments come from parametric down conversion in nonlinear crystals but we are instead opting to use FWM on Rubidium atoms since it allows for creation of two quantum correlated fields of similar frequencies. We use rubidium because it is an alkali atom with a single valence electron. Therefore, its spin can be optically aligned thus allowing the coherence of resonant properties instead of undesired spontaneous or incoherent emission. Due to hyperfine splitting in alkali atoms, a separation of ground states occurs, allowing us to optically address individual transitions.

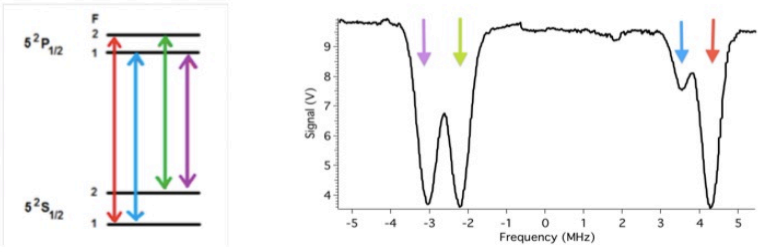

Figure 3: Relevant energy levels in Rubidium and the corresponding absorption spectrum

Many quantum information tools, based on coherent interaction of light with atoms and atom-like structures, suffer from bandwidth limitations that pose a challenge for interfacing with the crystal-based frequency-polarization Bell-states that contain short optical pulses of two very different optical frequencies[1]. The atom- based FWM will result in much smaller

frequency difference of the signal and idler fields which may bring them within reach of some recently proposed broadband quantum memory protocols with GHz bandwidth[4].

2 Experimental Framework and Optimization

2.1 Experimental Setup

This experiment uses a Titanium Sapphire laser to induce FWM. The laser is connected to the optical table via an optical fiber. The optical fiber is aligned such that about 40-45% of the power reaches the actual experiment. The laser is set to 400-420 mW as to allow for maximum power for inducing FWM without compromising the optical fiber. The cell is heated to 110° Celsius in order to optimize the FWM. The following demonstrates the optical equipment used in the experiment and their positions on the table.

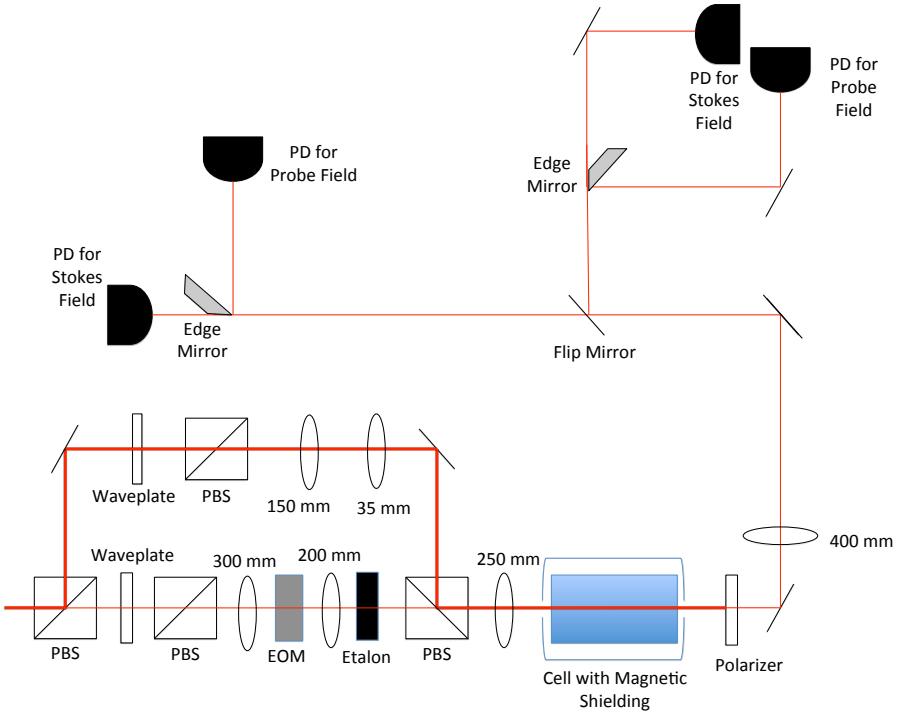

Figure 4: Original Experimental Setup.

The first polarizing beam splitter (PBS) separates the laser into two beams, the control

beam and the probe beam. The control beam has significantly more power than the probe beam. The control beam travels through a waveplate and another PBS set to maximum power flow for optimum results, another PBS, and two lenses prior to reaching the final PBS before traveling through the rubidium vapor cell. Since the probe field must have a frequency different from the control by the hyperfine splitting frequency of Rb atoms (approximately 6.835 GHz), we phase-modulate the weaker beam using an electro-optical modulator, and the use an etalon to filter out any other unwanted optical frequencies. The exact probe frequency is then controlled by an RF source, that determines the EOM modulator frequency. The two beams recombine in the PBS located in front of the Rubidium cell at a small angle. The recombined beams travel through the cell in which the interactions with the previously mentioned atomic transitions of rubidium cause FWM and produce two beams on the other side of the cell. For the purpose of simplicity, the two beams are shown as one in Figure 4. These two beams are the probe field, and its quantum correlated Stokes field. When using these photodiodes, the experiment uses the RF ramped from to 6827 MHz to 6877 MHz. The ramping function is responsible for the periodic behavior seen in Figure 5. In Figure 5, the data is visualized from a Matlab recorded image from the oscilloscope. Channel 1 is the Stokes field and channel 2 is the probe field.

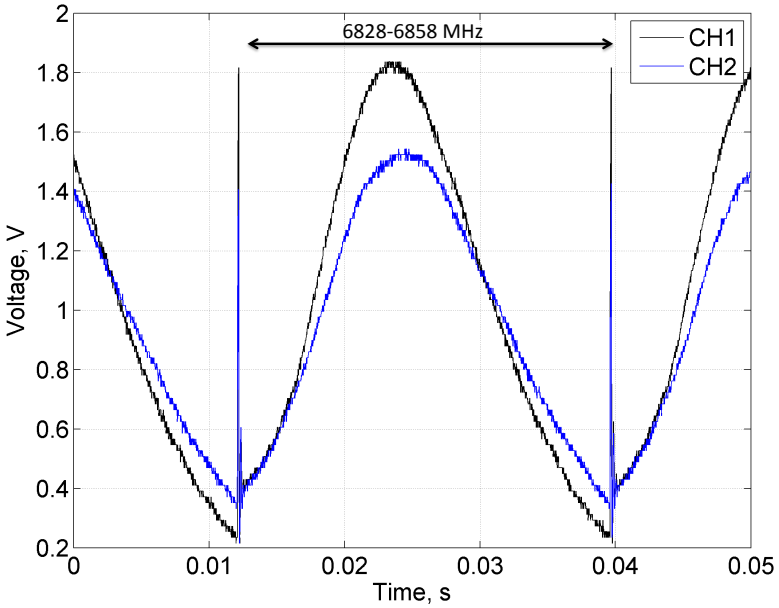

Figure 5: Raw FWM data

The flip mirror determines to which photodiodes the beams will travel. When the mirror is in use, the beams travel to the balanced photodiodes in the upper right corner of Figure 4. These photodiodes measure the differential intensity between the probe and Stokes field and is connected to a spectrum analyzer and are used for noise measurements. When the mirror is flipped down, the beam travels to the pair of photodiodes to the left in Figure 4. These photodiodes connect to oscilloscope and are used to measure the power of the probe and Stokes fields. These photodiodes were also used to analyze the optimization parameters discussed in the following section. Figure 5 shows the probe and Stokes field as shown through our oscilloscope at an optimized laser wavelength.

2.2 Optimization of Laser Tuning Four Wave Mixing

The laser must be tuned at a frequency close to the absorption frequency of Rubidium without actually hitting that frequency or else the light will completely absorb and there will be no FWM. In order to analyze which wavelength worked best. The signal through the oscilloscope was analyzed via MATLAB code that compared the probe field and Stokes field

to a reference recording containing no FWM. The measurements were made as a function of laser tuning and yielded the results in Figure 6. Figure 6 shows the gain of the Stokes and probe fields as a function of laser tuning.

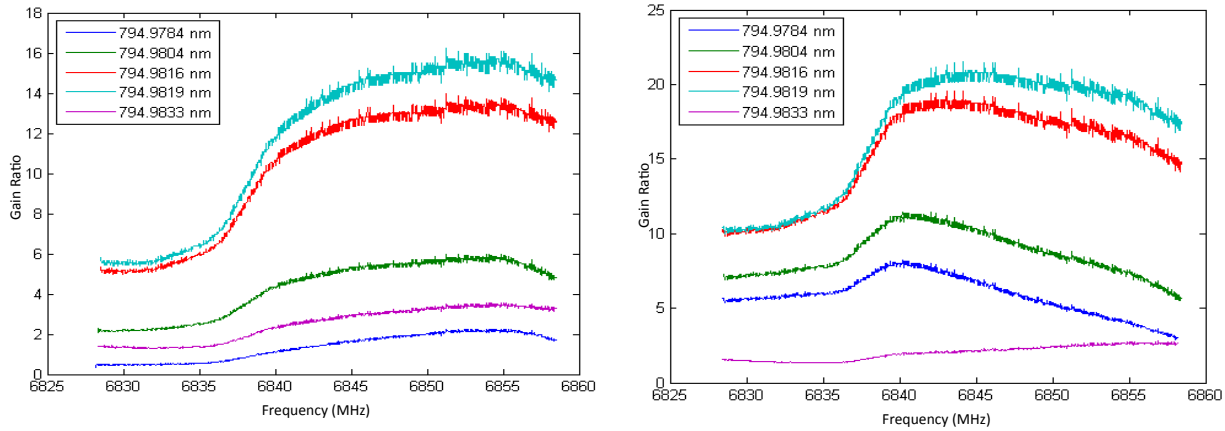

(a) Stokes Field Gain Profile

(b) Probe Field Gain Profile

Figure 6: The Gain Profiles

Fortunately, both the probe field and Stokes field showed maximum gain at the same wavelength of 794.9819 nm. Since the signal is similarly strong at 794.9816, this sets an acceptable range for the laser as it is nearly impossible for the laser to stay at one wavelength at such a precision. Further analysis established that as long as the wavelength stayed between 794.9815 nm and 794.9819 nm, the FWM would be strong enough to continue with the experiment.

3 Noise Measurements

3.1 Brief Introduction to Shot Noise

Shot noise is an intrinsic property of the light involved in this experiment. The term shot noise refers to the time-dependent fluctuations in electrical current. Shot noise exists due to discrete packets that move within the light and electric fields in the experiment. The

statistical distribution of shot noise resembles that of a Poisson Distribution [5]. For a coherent laser state, the shot noise should take the following form:

$$\delta I_{noise} \propto \sqrt{I_{laser}} \tag{3}$$

Where I_{noise} is the power of the noise and I_{laser} is the intensity of the laser. This equation mathematically explains the clear phenomenon that as the power increases, the noise will also increase.For the purpose of this report, shot noise will serve as a reference point for the experiment's other noise measurements since it is an intrinsic and expected property of the experiment. Shot noise is the classical reference and counterpart to the quantum noise ideally produced in this experiment.

3.2 Experimental Procedure for Measuring Noise

A parameter analyzer measures the noise in units of dB. The parameter analyzer is connected the the previously mentioned photodiodes responsible for noise measurements. The RF ramping function is turned off and the RF frequency is set to 6852 MHz for this portion of the experiment in order to keep the signal as constant as possible. In this experiment, the noise has been measured as a function of various parameters such as laser power, control field power, laser wavelength and frequency.

Obviously, the more power the system has, the more noise will be produced. However, without substantial power, FWM will not occur or have reliable results. The trick is to find the optimal power for both settings. The first step for the noise measurements was to determine the limit at which the amount of power saturated the photodetector and left the measurements invalid. The determined limit of saturation occurs when one photodiode reads around 475 or more μWatts of power.

3.3 Calibrating the Shot Noise

Once the power saturation level was established, the shot noise was measured at 1 MHz for a reference for all of our forthcoming noise measurements and analysis. The parameter analyzer has a Resolution Bandwidth (RBW) of 10 kHz and a Video Bandwidth (VBW) of 10 Hz. The following graph shows the measured shot noise as a function of power measured in one of the photodiodes. It does not matter which photodiode is used to measure power since ideally the power would be the same in both the Stokes and probe channels.

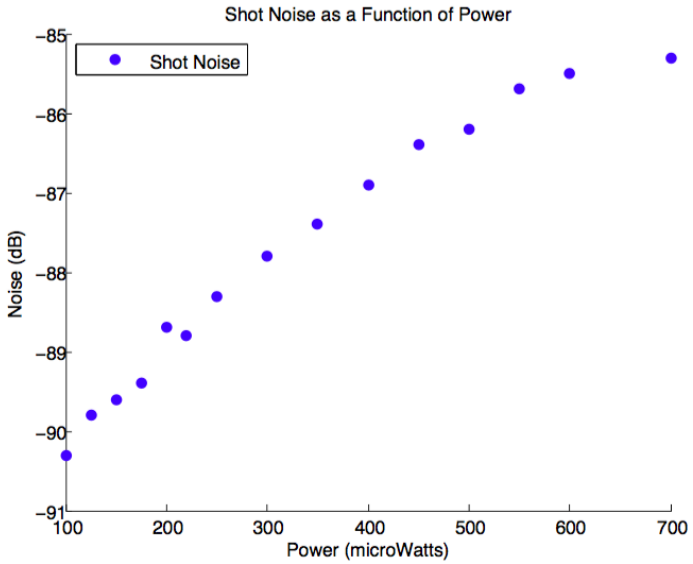

Figure 7: Shot Noise Graph

The shot noise graph shows the ideal noise the experiment should achieve at some setting that will be expounded upon in the following sections.

3.4 Settings for Optimized Quantum Noise

First, it is important to established a behavior pattern that is what would be expected since we believe that the intensity fluctuations in the probe and Stokes field are connected. It is expected that the noise will be lower when both photodiodes are opened and that the noise will increase when only one photodiode is open. The following image from the parameter

analyzer establishes this behavior.

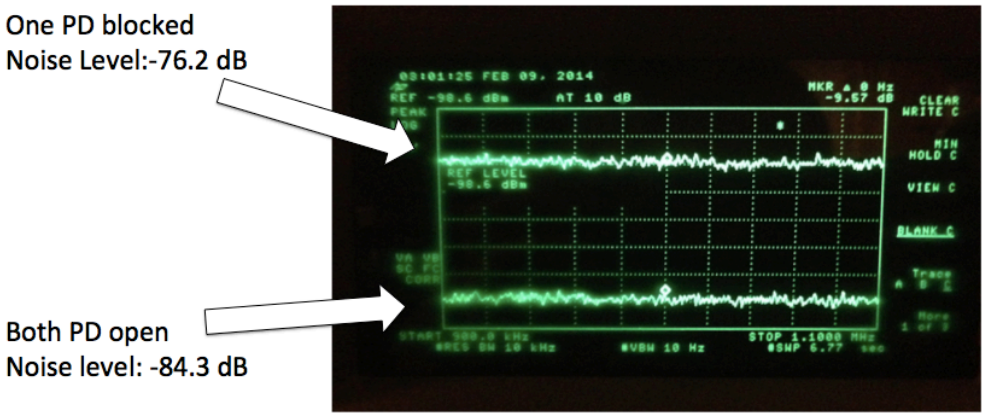

Figure 8: Noise behavior based on photodiodes

Since the noise behaves in the expected manner, the following sections show efforts to optimize the noise in an effort to match it to the shot noise.

3.4.1 Change in Set Up

After many trials that failed to reduce the measured differential noise to be closer to the shot noise, it was decided that the best course of action was to change the experimental setup to the arrangement shown in Figure 9.

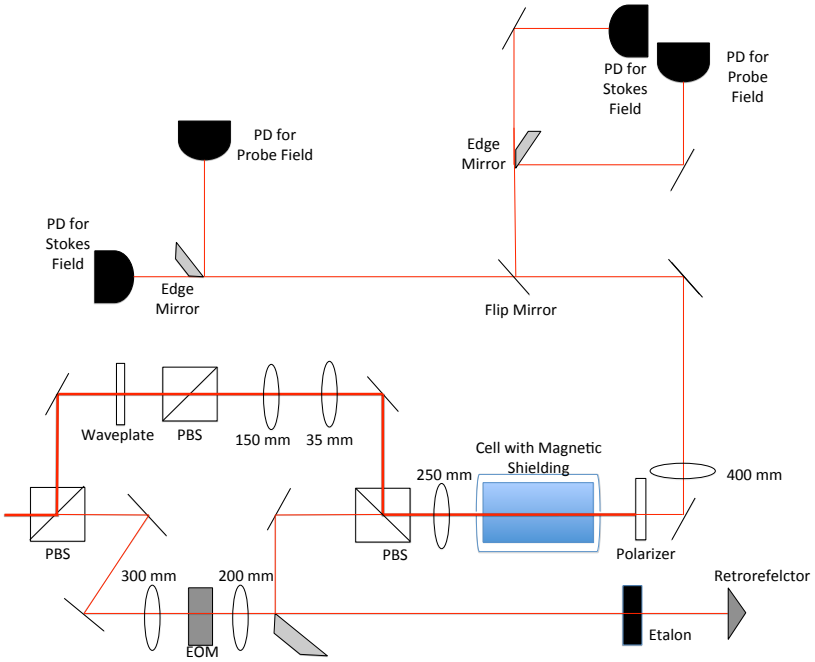

Figure 9: Updated Single Laser Setup

This change allow the probe beam to travel through the etalon twice in order to filter out any residual and undesired wavelengths in the light that could possibly contribute to the noise of the system. There was also an Iris placed in front of the PBS that combines the beams before traveling through the cell. This iris decreased the diffraction that was becoming noticeable and likely contributing to the high noise.

3.5 Matching the Shot Noise

After numerous trials adjusting the control field power, laser power, and laser wavelength, the noise as a function of power dependent on the RF source frequency was tested. For all of these trials, the RF source was set to 6852 MHz based on the known transitions of the Rubidium. When adjusting the RF to higher frequencies, the noise increased. However, when adjusting the RF to lower frequencies, the noise decreased from the previous measurements. These measurements yielded the following results when compared to the shot noise:

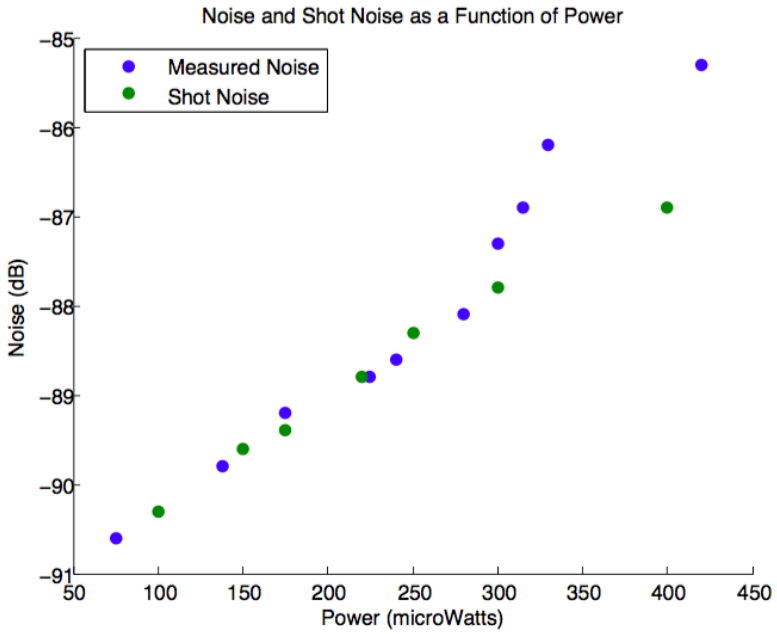

Figure 10: Noise measurments compared to the shot noise

The shot noise matches the measured noise at about 265 and 225 μWatts which corresponds to an RF source of 6846 and 6844 MHz respectively.

4 Noise Optimization for Two Phase Lock Lasers

4.1 Two Laser Setup

Although in the previous stages there points at which the shot noise limit was matched, to further establish quantum correlation we must see noise levels that are solidly below the shot noise. Since the shot noise limit was reached with the previous set-up but not optimal, a change in the experimental set-up was made. Instead of both the control field and the probe field coming from the Titanium-Sapphire laser, the new setup has the control field coming from the Titanium-Sapphire laser and the probe field generating from an external cavity diode laser. We made this change to the two laser setup because with the single laser setup, we were unable to completely eliminate the control frequency from the probe field by using

the etalon. Our hope is that without the leak of the control into the probe field, we will be able to achieve noise lower than the shot noise limit.The following two diagrams show the new beam paths of each field before recombining into the rubidium cell.

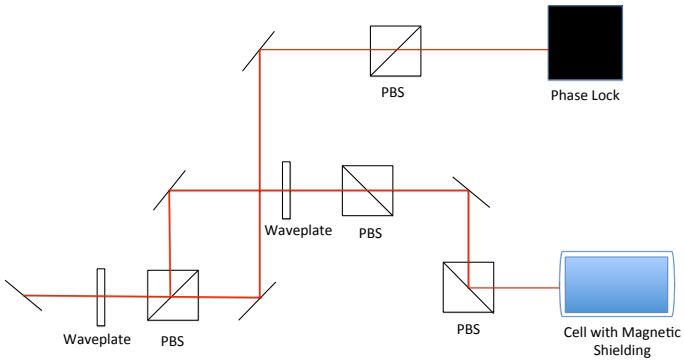

Figure 11: The path of the control beam supplied by the Titanium-Sapphire laser

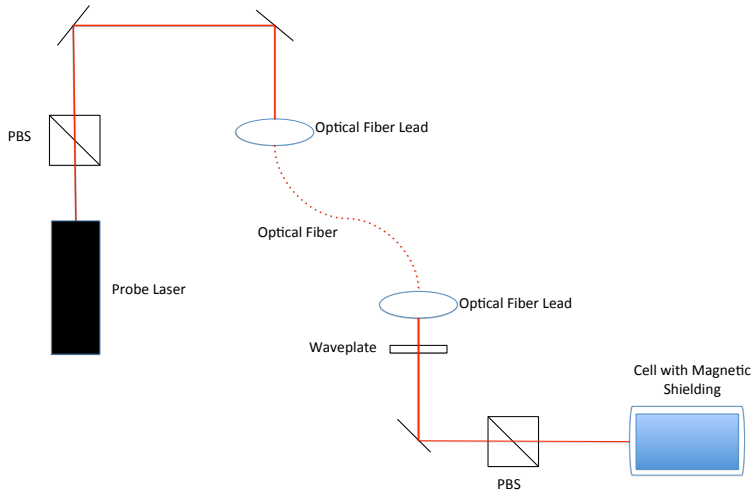

Figure 12: The path of the probe beam. The laser for the probe beam is located on the same table as the experiment.

The setup following the FWM inside the cell remained the same as in previous figures

with two photodiodes for noise analysis, and two photodiodes for spectra analysis.

4.2 Optimizing the Laser Settings

With the new set up, it became necessary to check the optimal wavelength for the control laser once again. This also became easier with the help of a new program that better stabilizes the wavelength of the Titanium Sapphire laser. Although there was a slight variation in optimal wavelength from 794.9819 nm to 794.9816 nm, the range of 794.9815 to 7794.9819 remained a valid parameter from the control laser.

The frequency of the probe beam before was set by an RF source. The phase lock frequency for the probe field is now set by a generator. Before continuing, it was important to find the frequency that would result in the lowest possible noise while still maintaining a high enough signal in the photodetectors to produce viable data. The following figures show the results of these measurements. The following figures show the result of these measurements.

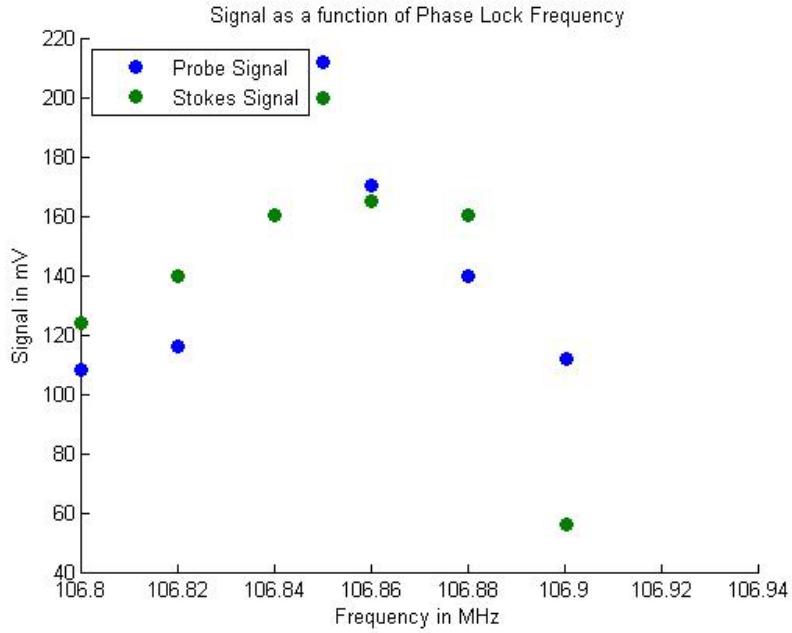

Figure 13: Probe and Stokes power as a function of phase lock frequency from 106.8 MHz to 106.9 MHz

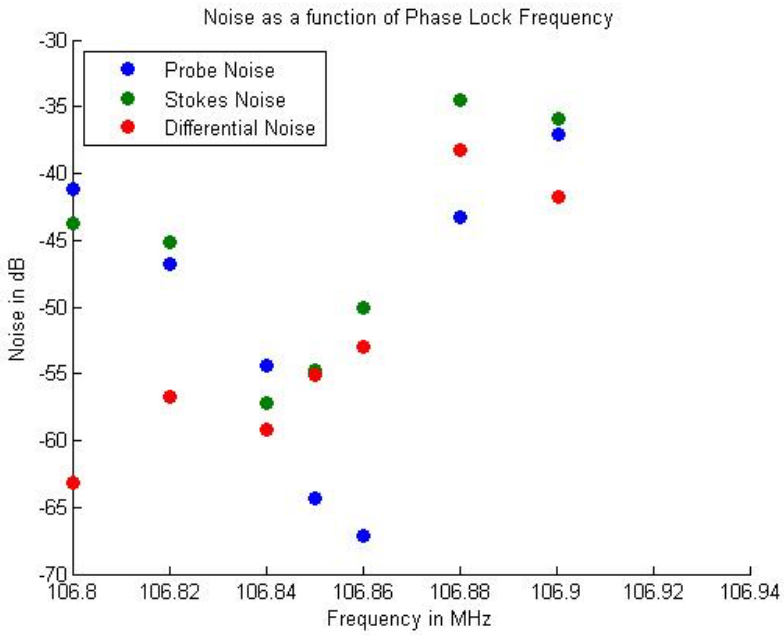

Figure 14: Noise as a function of phase lock frequency from 106.8 MHz to 106.9 MHz

The signal is mostly consistent with the exception of two outliers at 106.5 MHz and 106.9 MHz where in the latter the signal hits off resonance. The noise is lowest around 106.85 and 106.86 MHz thus those are our optimum frequencies. Noise in the probe and stokes field individually is expected to be higher than the differential noise. This graph shows the correlation we would expect

4.3 Quantum Correlation

With the new setup, the following noise spectrum was observed

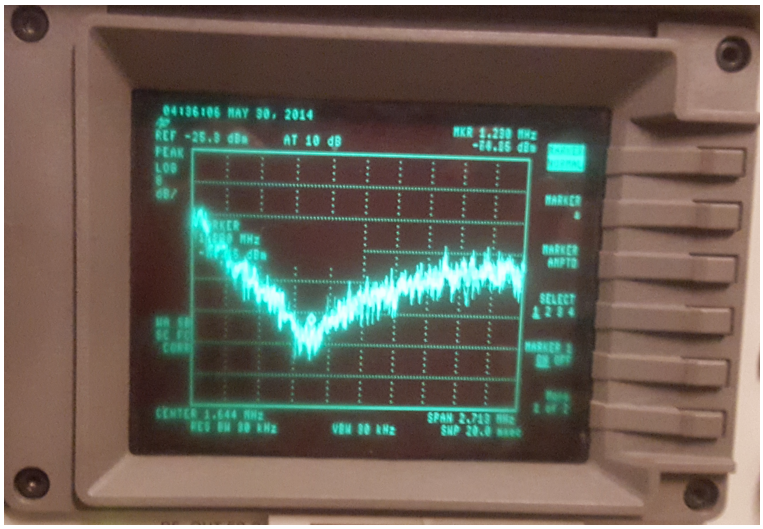

Figure 15: Noise Spectrum

This dip in the noise spectrum shows clear quantum correlation in the experiment. The dip is the closest signal to reaching below the shot noise limit observed so far. This closeness to the shot noise shows promise for the double laser configuration. However, this noise reading is still above the shot noise limit thus there are still many potential improvements in the system.

4.4 Testing Loss in the System

When approaching the shot noise limit, it is important to eliminate as much loss as possible in the system in order to obtain the most accurate noise measurements. The first step in decreasing the loss was to create a more direct path to the the photodiodes that link to the spectrum analyzer. The following figure shows the change in the setup with hopes of reducing loss.

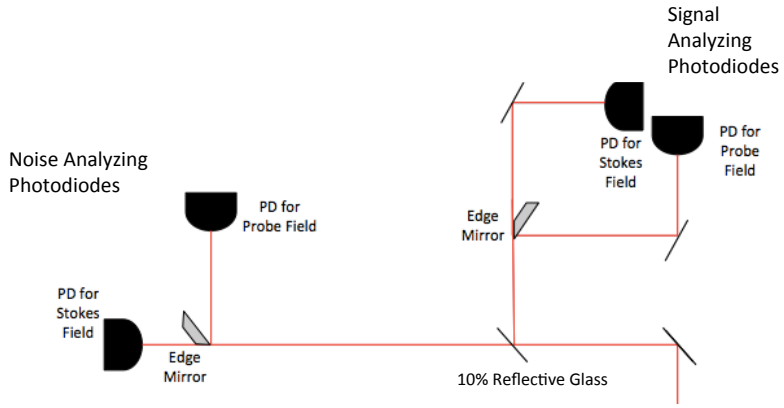

Figure 16: Setup for less loss in the noise analysis

Now the path to the noise analyzing photodiodes has less interruption than in the previous setup as the beams only reflect off of one mirror then the edge mirror as opposed to reflecting off of two mirrors before reaching the edge mirror. We hoped that the reflective glass would make the system loss less and allow us to analyze the noise and the signal at the same time. Although we can still use the mirror to make sure the signal and noise analysis appears compatible, the noise difference with an without the glass was significant due to some clipping of the beams as they increase in size along their path. Therefore, the mirror must be removed from the beam path during noise measurements

4.5 Importance of Probe Laser Lock

One of the more important discoveries during the noise improvement work was the effect of the location at which the probe laser locks. The probe laser often goes out of phase and the frequency must be adjusted to re-lock the laser. When this is done the frequency at which the laser is locked changes. It was originally thought that this would not have a substantial effect on the noise in the system. However, when measuring parameters such as noise and

signal as a function of power or noise and signal as a function of control laser wavelength, the measured parameters had less of an effect than the adjustments of the laser lock as the laser lock drifted in and out of place. For example, during one trial of noise as a function of power, there were 3 measurements where the control power was 140 mW. For this specific power, there were three levels of noise recorded: -71 dB, -48 dB, and -63 dB. The only parameter that changed between these measurements was the location of the laser lock. Similar results were observed when measuring noise and signal as a function of the previously mentioned parameters.

4.6 Installing a New Control Laser

Reviewing some of the previous work on FWM in Rubidium, it is clear that most experiments use a higher power laser [6]. Since the Titanium Sapphire laser is on table separate from the experiment, an optical fiber must be used. However, for a single mode optical fiber, no more than 500 mW can safely run through the fiber allowing a theoretical maximum power of only 250 mW for the control beam. By having a more powerful laser in future work, the likelihood of improving the current results increases. In addition, much of the noise in both the single laser and double laser configuration was attributed to excess noise caused by the titanium sapphire laser. Installing a new laser would ideally improve both critical issues at once. The new laser was just installed and the ideal wavelength range is between 794.9815 nm and 794.9819 nm, which matches the optimal wavelength range of the titanium sapphire laser.

4.6.1 Analysis of the Laser Lock Gain

Additionally, we analyzed the coarse gain function of the laser lock system. We did this to see if there was an alternate source for the noise outside of the noise of the titanium sapphire laser. The noise for the new control laser looked very similar to that of the noise with the titanium sapphire laser, thus the possibility exists for other causes of noise. There were some

trials taken with the lock turned off, and some trials taken at different noise levels of coarse gain.

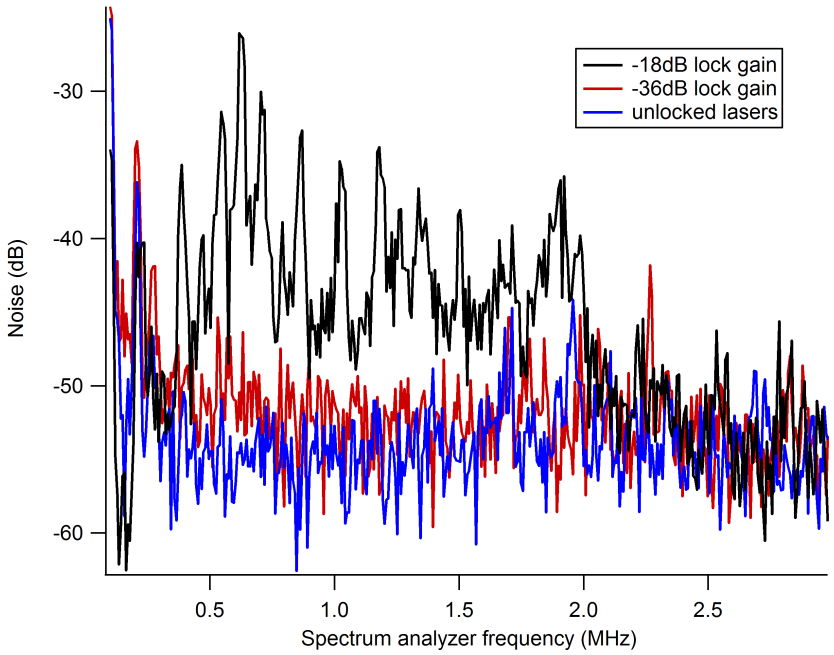

Figure 17: Noise measurements with a constant DC signal

From Figure 17, it is clear that when locked at -36 dB, the noise is consistent with the reading without the lock. It is important to also note that the DC signal in the noise photodiodes was constant and around -280 mv. The graph shows that the lock works as intended and does not have a negative impact on the noise reading.

4.6.2 New Parameters for Control Field

Although we established the optimal wavelength for the control laser, with the new laser we must also find the new optimal settings for the probe laser. The probe laser frequency was analyzed and the results are shown in the following figure.

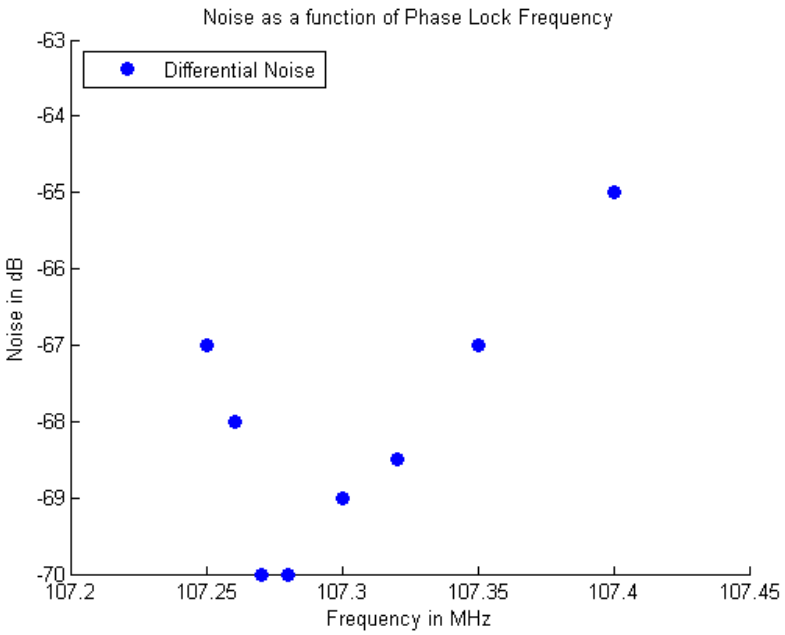

Figure 18: Differential, Probe, and Stokes Noise Readings

We can see that the new setting for the probe laser is at 107.28 MHz as that location produces the lowest noise reading. After establishing the settings, we analyzed the full spectra of the noise.

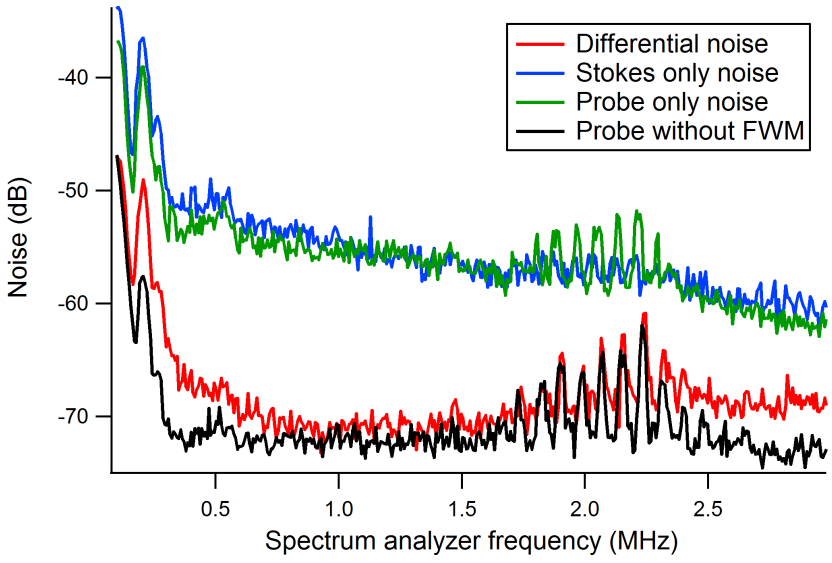

Figure 19: Differential, Probe, and Stokes Noise Readings

Figure 18 shows noise that is behaving as expected and getting lower. We expect that

the Probe field and the Stokes field will have higher noise than the differential noise. The Differential noise is about -70 dB meaning that we are getting closer to the shot noise limit with the double laser configuration. Around 2 MHz, there is visible oscillation that at first we were unable to explain. It was later shown that the oscillations in the noise are caused by the temperature controller of another experiment in the lab. Therefore, when taking noise measurements on this experiment, it is crucial to cease function on the other experiment.

4.6.3 Increasing the Control Laser Power

One of the larger benefits of the new control laser is the potential to increase the control power through the Rubidium vapor cell past the previous maximum of 135 mW. After optimizing the noise at 135 mW, we increased the control power to 280 mW. With the higher power came larger beams so we put irises in the path of the beam before the noise reading photodiodes. These irises had to be adjusted precisely and in conjunction with each other to reach the lowest possible noise achievable in the set up. Closing one iris too much while leaving the other more open results in drastic increases in noise as is demonstrated in Figure 19. The increase in power and iris placement proved to be successful as the noise hit -80 dB, which is about 5 dB away from the shot noise limit. What was more difficult at this stage was finding the optimal frequency for the probe laser. In previous measurements, the frequency that produced optimal noise readings was a fairly small range. At this power, frequencies that are 0.5 MHz apart can still have the same noise reading. The following figures show signal measurements of both the Probe and Stokes fields at a range of frequencies that all show the same noise reading of -80 dB

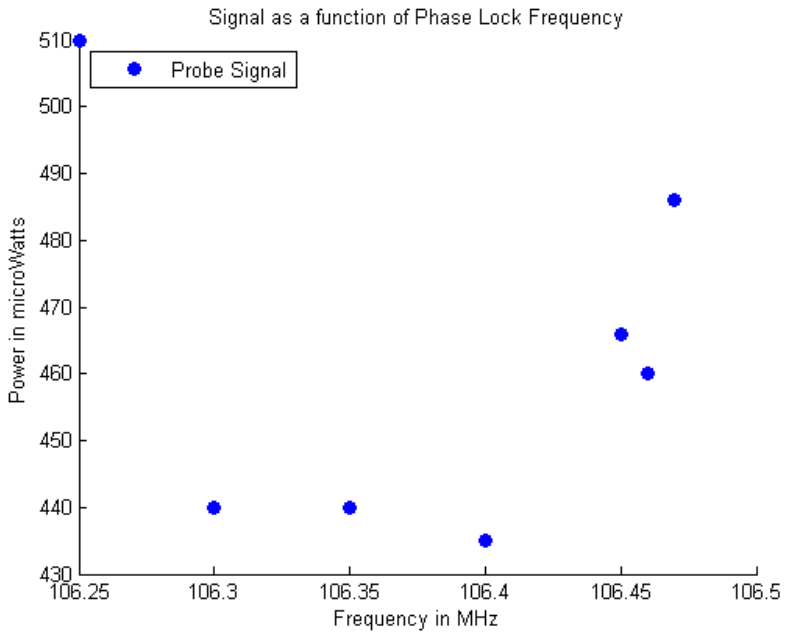

Figure 20: Probe power as a function of Phase Lock Frequency

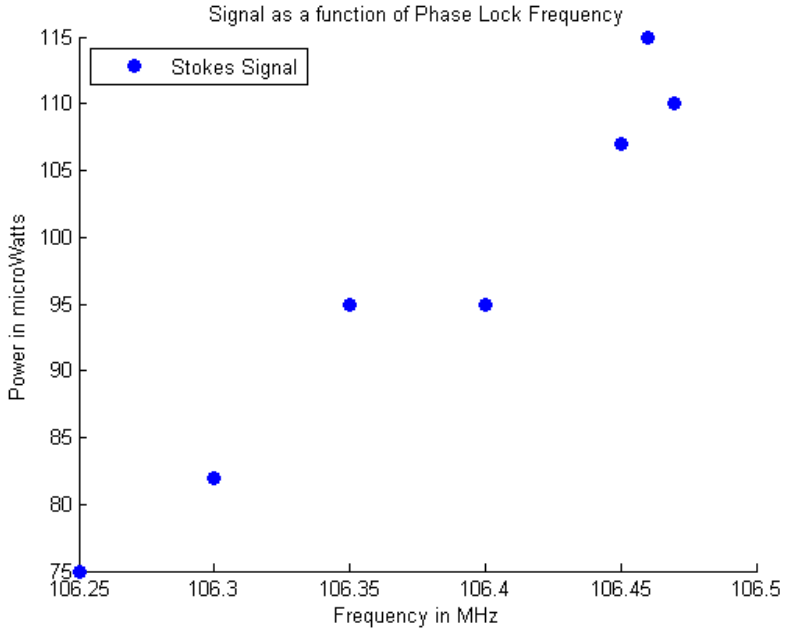

Figure 21: Stokes power as a function of Phase Lock Frequency

From this set of data, we can see that the optimum frequency is 107.46 MHz as that is where the Stokes field has the highest power. The probe field is already very high so it is more important that the Stokes signal be high enough to show valid results from the FWM.

5 Conclusions and Future Work

5.1 Conclusions

Light entanglement holds promise in the field of quantum information and quantum sensor technology. In the first semester, the optimum settings for FWM mixing were established for a system with one laser creating both control and probe fields. We then began noise measurements for this setup including calibrating the shot noise limit which would become our ultimate reference in establishing the quantum activity in the system. We then changed the setup to include a double passing in an etalon but the noise was ultimately non optimal in the single laser setup. We then switched to a double laser setup with the control field produced still by the titanium sapphire laser and the probe field produced by a different and less powerful infrared laser. Some progress was made in improving the noise in this setup, but a new control laser was installed that would give more promise by having a higher power and potentially having less noise than the titanium sapphire laser.

5.2 Future Work

In upcoming work, we will ideally find parameters that will allow the quantum noise to be below the shot noise at multiple points. There is still a lot of optimization to occur with the new control field laser and establishing how it best functions with the lock and the probe laser. Solidifying these parameters will further establish the quantum correlation between the probe and stokes field and will show that the potential for creating entangled Bell States exists.

5.2.1 Incorporating the Polarizing Apparatus

Once the quantum correlation is truly established, the goal is to induce the polarization of the Bell states. It is through polarization that the Bell states will be filtered and able to be analyzed. A project completed last year will be used as a low-loss frequency-selective

polarization controller. This polarization controller uses the linear Faraday effect in presence of a magnetic field to induce the necessary polarization to create the polarized entangled Bell states. Mathematically, the Faraday effect can be demonstrated by the following equation

$$\beta = \nu B d \tag{4}$$

Where β is the angel of rotation it radians, B is the magnetic flux density, d is the length of the path in meters, and ν is the verdet constant of the material. The following figure shows how the Faraday effect works in a solenoid like the one used in this experiment.

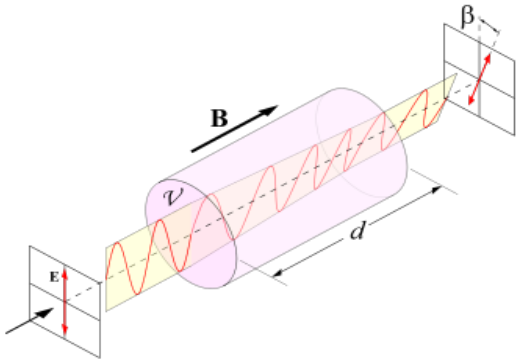

Figure 22: Visualization of the Faraday Effect

The goal of this project was to utilize the Faraday effect to produce a polarization that would completely rotate the light traveling through the rubidium vapor cell. It was initially estimated that the desired magnetic field needed to reach full rotation was around 20-30 Gauss. The following apparatus was then built.

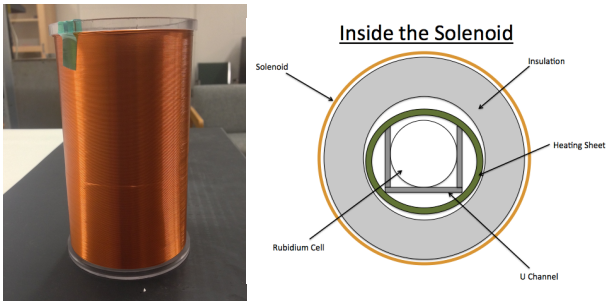

Figure 23: Faraday Solenoid

The solenoid is made from copper wire through which we apply a current. Within the solenoid is insulation to prevent the exterior from overheating, heat sheets to provide the heat necessary fro the complete rotation, and a U channel that holds the rubidium vapor cell. Although we previously thought that approximately 20 Gauss would induce full rotation, after many trials and parameter adjustments, we found that the necessary magnetic field (and therefore the necessary current) was approximately double the estimated amount. Figure 23 shows the rotation results that occur when adding the higher magnetic field.

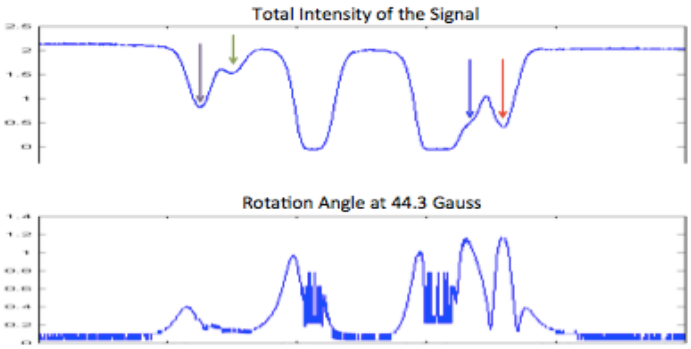

Figure 24: Rotation Data with 44.3 Gauss

The full rotation occurred with a current of 44.3 Gauss which required a current input of close to 2 amps. To achieve this current input, we had the couple a power source. Using this apparatus will allow us to produce the polarization Bell states via full rotation once the quantum correlation is completely established.

6 Acknowledgements

I'd like to thank Irina Novikova for her excellent guidance in this project. Additionally I'd like to thank Nathan Super for his work on the Titanium Sapphire wavelength control program.This work is supported by National Science Foundation under grant No. PHY-308281 and the Virginia Space Grant Consortium.

References

[1] T. S. Iskhakov, I. N. Agafonov, M. V. Chekhova, G. O. Rytikov, and G. Leuchs. *Polarization properties of macroscopic Bell states* (PRA 84, 045804, 2011)

[2] D. Dehlinger and M. W. Mitchell. *Entangled photons, nonlocality, and Bell inequalities in the undergraduate laboratory* (Physics Department, Reed College, Portland Oregon, 2001)

[3] R. Paschotta, *four wave mixing* (Encyclopedia of Laser Physics and Technology, 1. edition October 2008, Wiley-VCH, ISBN 978-3-527-40828-3)

[4] I. Novikova, *Generation of macroscopic optical polarization Bell states in atomic ensembles via four-wave mixing* (2012)

[5] M. de Jong, *Sub-Poissonian shot noise* (Physics World, August 1996, pg 22)

[6] M. Turnbull, *Multi-Spatial-Mode Quadrature Squeezing from Four-Wave Mixing in a Hot Atomic Vapor* (University of Birmingham, August 2, 2013)